Multi-dimensional LOCA Analysis, Status and Perspective

Sang Yong Lee [a*]
[a]*KEPCO International Nuclear Graduate School,*
658-91 Haemaji-ro Seosaeng-myeon Ulju-gun, Ulsan 689-882, Republic of Korea
[*]*Corresponding author: sangleey@kings.ac.kr*

1. Introduction

Korea Realistic Evaluation Model (KREM) basically follows Code Scale Applicability and Uncertainty (CSAU) [1] methodology. Since KREM was approved by the Korean authority in 2002, it has been applied to support several important domestic and foreign projects such as APR-1400 (Advanced Power Reactor) design, APR-1400 export to United Arab Emirates (UAE) and U.S. NRC design certification of APR-1400.

The phenomena of Loss of Coolant Accident (LOCA) have been investigated for long time. And the most extensive research project for LOCA was the 2D/3D program [9]. It involved large or full size experiments such as CCTF (Cylindrical Core Test Facility), SCTF (Slab Core Test Facility) and UPTF (Upper Plenum Test Facility) as well as the most up-to-date two-fluid analysis code, TRAC [3].

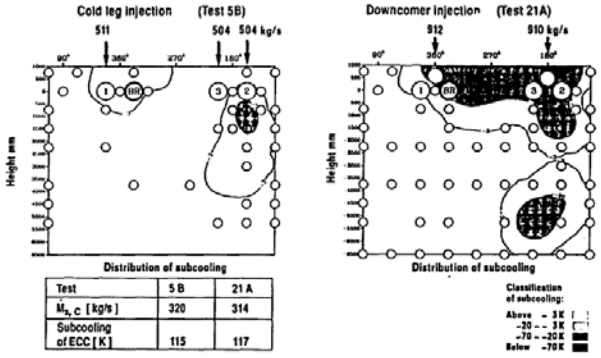

Test	5B	21A
$\dot{M}_{s,c}$ [kg/s]	320	314
Subcooling of ECC [K]	115	117

Fig.1. Flow Pattern in Downcomer

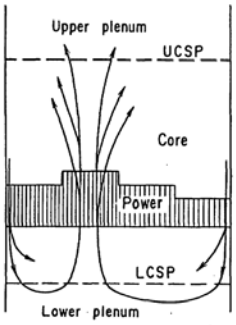

Fig.2. Flow Distribution in Core during Reflood

With the background of 2D/3D study, the topic of this paper is to investigate facts concerning LOCA application of the present day up-to-date code systems such as RELAP5[6], TRAC, CATHARE [8] and COBRA-TF [2]. Especially, focus has been put on the multi-dimensional phenomena.

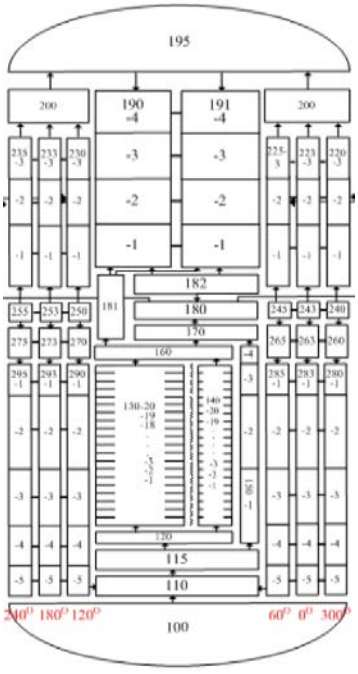

Fig.3. RELAP5 Noding scheme of Vessel in KREM

2. Multi-dimensional Approach to LOCA

2.1. Summary of the results of 2D/3D experiments

The results of the 2D/3D experiments are summarized as follows;

Flow conditions in the downcomer during end-of-blowdown were **highly multi-dimensional at full-scale** (Fig.1). During reflood, the distribution of water in the core was one-dimensional. But flow in the core exhibited multi-dimensionality (Fig.2). One-dimensional manometer oscillation between the downcomer and core was observed. The water level was higher in front of the broken cold leg nozzle than at other azimuthal positions. Flow phenomena at the tie plate were uniform.

2.2. Multi-dimensional treatments in KREM

KREM heavily relied on the results of the 2D/3D research project. They were main sources of the back-up information to justify using RELAP5 for LOCA analysis. As shown in Fig.3, downcomer has six channels with cross flow junctions. Each channel

matches with a main coolant loop pipe. The multiple channels with cross flow junctions construct a flow network around downcomer. The deficiency of the flow network approach is evaluated by assessing the full size experiment, UPTF-4A for the downcomer behavior during End of Blowdown (EOB). The discrepancy between the experimental result and the calculation result are quantified and used to assess the bias. The bias for the level depletion during reflood period is assessed with UPTF-25A.

Reactor core has two channels with cross flow junctions. One of them is for a hot assembly and the other one is for the rest of assemblies. As explained in section 2.1, multi-dimensional effects in core mainly help the core cooling. The chimney effect and the cross flow between hot and cold channels (Fig.2) are most important phenomena. The applicability of 2 channel approach is evaluated using LOFT/L2-5.

2.3. Multi-dimensional Analysis in TRAC/CSAU

Fig.4 illustrates the selected cell definition. The reactor vessel has been modeled with three radial rings, four azimuthal sectors, and 15 axial levels, for a total of 180 fluid cells. In addition, the guide tubes have been modeled by eight one-dimensional pipe components with five cells per tube, requiring an additional 40 cells.

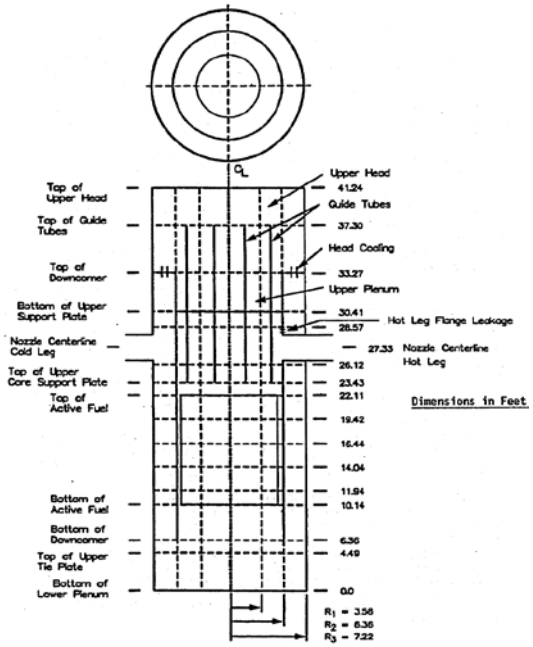

Fig.4. Noding scheme of Vessel in TRAC/CSAU

Four azimuthal sections were selected for the plant model, preserving symmetry and minimizing impact on calculated peak cladding temperature. The axial level division chosen uses ten axial divisions in the downcomer. The lower plenum nodding contains three axial levels. The calculation must account for multi-dimensional flow, hot walls, and lower plenum voiding (sweep-out). The upper plenum is defined as the region between the top of the active core and the top of the reactor vessel. The region above the core is therefore modeled with seven axial zones, three radial rings, and four azimuthal sections. The fuel region of the vessel model is divided into five axial regions and two radial rings, with four azimuthal sectors. Supplemental fuel rods are added to the core model as required for sensitivity and uncertainty calculations.

The deficiency of TRAC code during the EOB time was treated as a bias. UPTF-6 and other scaled tests were used to estimate the bias.

2.4. Multi-dimensional Analysis with CATHARE

CATHARE 3 has the capability to use multi-3D approach with local refinement. One of the objectives of CATHARE 3 is the modelling of a PWR pressure vessel by means of several 3D modules assembling lower plenum, heating core, bypass, downcomer, upper plenum and upper head (Fig.5).

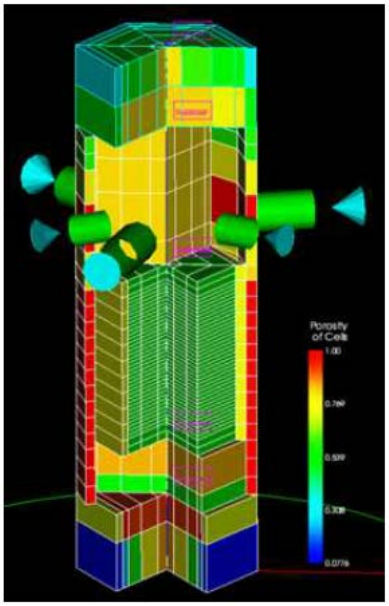

Fig.5. Noding scheme of Vessel in CATHARE

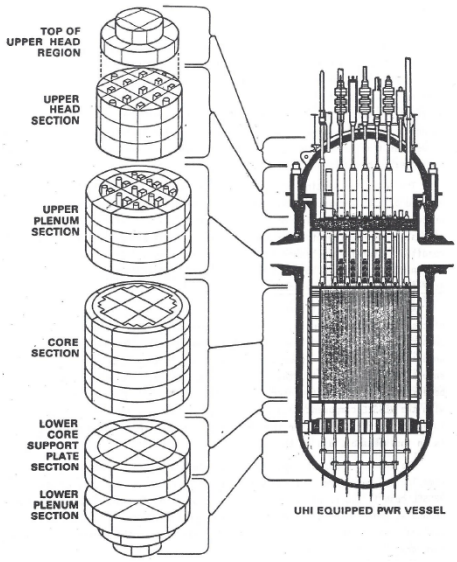

Fig.6. Noding scheme of Vessel in COBRA-TF

This will make it possible to refine one zone independently from the other, adding the possibility to use non-conforming junctions to connect various 3D elements. It will also make it possible to use a more adapted system of coordinates to describe each zone of the vessel, as for instance spherical coordinates for the lower plenum, cylindrical ones for the annular downcomer and the upper plenum, Cartesian ones for the core, etc.

2.5. Multi-dimensional Noding with COBRA-TF [2]

Examples of reactor vessel regions formed by specifying channels and inter-channel connections (gaps) are shown in Fig.6. The basic building block for the vessel mesh is the channel; that is a vertical stack of single mesh cells. Several channels can be connected together by gaps to model a region of the reactor vessel. Regions that occupy the same level form a section of the vessel. Vessel sections are connected axially to complete the vessel mesh by specifying channel connections between sections. Heat transfer surfaces and solid structures that interact significantly with the fluid can be modeled with rods and unheated conductors.

3. Reviews on the Momentum Equations

3.1. Momentum equations in various forms

The multi-dimensional effects are simulated with the proper treatment of the momentum flux term in the momentum balance equations. Various modifications and/or simplifications are made to implement the solution schemes for the individual codes. Table-1 shows such variations.

Time and volume averaged porous body mass and momentum equation for phase k are written [10,11,12];

$$\frac{\partial \epsilon \alpha_k \rho_k}{\partial t} + \nabla \cdot (\epsilon \alpha_k \rho_k \boldsymbol{v}_k) = \epsilon \Gamma_k \quad (1)$$

$$\frac{\partial \epsilon \alpha_k \rho_k \boldsymbol{v}_k}{\partial t} + \nabla \cdot \left(\epsilon C_{v_k} \alpha_k \rho_k \boldsymbol{v}_k \boldsymbol{v}_k\right) = -\epsilon \alpha_k \nabla p + \epsilon K_k \rho v^2 \ldots \quad (2)$$

The porosity is assumed 1.0 because it is not important for the following discussions. Then, momentum balance equation for phase k is written as;

$$\frac{\partial \alpha_k \rho_k \boldsymbol{v}_k}{\partial t} + \nabla \cdot \left(C_{v_k} \alpha_k \rho_k \boldsymbol{v}_k \boldsymbol{v}_k\right) = \alpha_k \nabla p + K_k \rho v^2 \ldots \quad (3)$$

The momentum loss due to the flow resistance (the wall friction plus the form loss) is usually correlated with total velocity head ρv^2 and proper phase partitioning factor. So, K_k implies the properly phase partitioned resistance factor.

The covariance coefficient, C_{v_k}, reflects the volume fraction distribution across the averaging volume. If operator $[[\star]]$ defines volume averaging of variable $\star$ and $\langle\langle\star\rangle\rangle$ means $\frac{[[\alpha_k \star]]}{[[\alpha_k]]}$, then, it is expressed as [10];

$$C_{v_k} \equiv \frac{\langle\langle \boldsymbol{v}_k \boldsymbol{v}_k \rangle\rangle}{\langle\langle \boldsymbol{v}_k \rangle\rangle \langle\langle \boldsymbol{v}_k \rangle\rangle} \quad (4)$$

It was studied for the one-dimensional pipe flow [11,12]. It is not generally 1.0. This is also true for general porous body multi-diemsional multi-fluid flow. But most of the present codes assume;

$$C_{v_k} = 1.0 \quad (5)$$

With this assumption, non-conservative form can be derived by expanding eqn.(3) and using mass conservation equation, eqn.(1);

$$\alpha_k \rho_k \frac{\partial \boldsymbol{v}_k}{\partial t} + \alpha_k \rho_k \boldsymbol{v}_k \cdot \nabla \boldsymbol{v}_k = -\alpha_k \nabla p + K_k \rho v^2 - v_k \Gamma_k \ldots \quad (6)$$

The phase intensive equation is written;

$$\frac{\partial \boldsymbol{v}_k}{\partial t} + \boldsymbol{v}_k \cdot \nabla \boldsymbol{v}_k = -\frac{1}{\rho_k} \nabla p + \frac{K_k}{\alpha_k \rho_k} \rho v^2 - \frac{v_k \Gamma_k}{\alpha_k \rho_k} \ldots \quad (7)$$

The immediate problem with these equations is that discretizing the eqn.(6,7) in finite volume method is not easy. To overcome this problem, Weller [15] used the modified non-conservative momentum equations as follows;

$$\boldsymbol{v}_k \cdot \nabla \boldsymbol{v}_k \equiv \nabla \cdot (\boldsymbol{v}_k \boldsymbol{v}_k) - \boldsymbol{v}_k (\nabla \cdot \boldsymbol{v}_k) \quad (8)$$

Next problem of eqn.(6,7) is that the estimated momentum fluxes with them are not correct because they are not reflecting mass fluxes correctly. To overcome these problems, the mass weighted modified non-conservative method [4] is used. In that, the following equality is used.

$$\alpha_k \rho_k \boldsymbol{v}_k \cdot \nabla \boldsymbol{v}_k \equiv \nabla \cdot (\alpha_k \rho_k \boldsymbol{v}_k \boldsymbol{v}_k) - \boldsymbol{v}_k (\nabla \cdot \alpha_k \rho_k \boldsymbol{v}_k) \quad (9)$$

The manipulations in eqn.(6,7) is totally relied on the assumption eqn.(5. If this is not held, the following equation is derived;

$$\alpha_k \rho_k \frac{\partial \boldsymbol{v}_k}{\partial t} + C_{v_k} \alpha_k \rho_k \boldsymbol{v}_k \cdot \nabla \boldsymbol{v}_k + \boldsymbol{v}_k \nabla \cdot \left(\left(C_{v_k} - 1\right) \alpha_k \rho_k \boldsymbol{v}_k\right) = -\alpha_k \nabla p + K_k \rho v^2 - v_k \Gamma_k \ldots \quad (10)$$

It means that the non-conservative form is not available. Therefore, the non-conservative form of momentum equations for the time-volume averaged on porous body should not be constructed.

3.2. Order of magnitude of the momentum flux term

The importance of the momentum flux term should be evaluated against the resistance term. It is evident that the momentum flux term is solely important for the non-porous body (or open body) problem.

The resistance term in the core flow of a typical pressurized water reactor is usually very much larger (>10.0) than the momentum flux term because of the packed fuel rods with spacer grids. Therefore, the importance of the momentum flux term is relatively weak. This is also true for the lower plenum flow and for the upper plenum flow considering the internal structures in them.

This is not evidently true for the flow in downcomer. Considering the curvature of the downcomer, the form loss factor of single phase flow is estimated to be about

1.0. The momentum flux term is about 1.0 as well. Therefore, relative importance of the momentum flux term is determined by the two phase multiplier. Martinelli-Nelson average two-phase friction multiplier for 1.0 % quality at 5.0bar is about 2.0. Therefore, it is concluded that the momentum flux term is important in downcomer flow.

Table-1. Treatment of Momentum Equation in Codes

	RELAP5	TRAC TRACE	CATHARE	COBRA-TF
Dim.	1-D	3-D	3-D	3-D
Eqn.	Non-conservative	Non-conservative	Modified non-conservative	Conservative
Phase	Mass weight (sum eqn.) Phase int. (diff. eqn.)	Phase intensive	Mass weight	Regular
Geometry	Network	Cylindrical	Cyl/Sph/Rect	Rect
Mesh	FVM	FDM	FVM	FVM

3.3. Treatment of momentum flux term in codes

To solve for the velocity, many codes use non-conservative form of momentum equation (Table-1). TRAC and TRACE [13] use the phase intensive momentum equation like eqn.(7). Finite difference method is applied to discretize the momentum equations in TRAC and TRACE. It is not possible to estimate the momentum flux correctly in this code as already explained in section 3.1. Fig.7 shows the situation in that wrong estimation of momentum flux may happen.

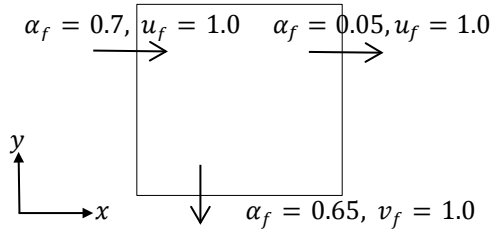

Fig.7. Flow Configuration of a Cell

Knowing this problem, CATHARE use the modified non-conservative, mass weighted form like eqn.(9). Since the momentum equations can be represented nearly conservative form in this approach, finite volume method is naturally adopted for their discretization. Some accuracy loss is inevitable to discretize the $\boldsymbol{v}_k(\nabla \cdot \alpha_k \rho_k \boldsymbol{v}_k)$ term of eqn.(9) because it is not fully conservative. But, this approach is valid only with the very unnatural correlation (eqn.(5)).

COBRA-TF use regular conservative momentum equations like eqn.(3). And it solves for the momentum flux. It also uses the covariance correlation eqn.(5). Discretization of the conservative momentum equations through the finite volume method is rather straightforward. Unlike the non-conservative equation, second order accuracy of the discretization can be kept.

If all the cross momentum convections are assumed dissipated at the highly porous plates such as fuel bottom nozzle and fuel top nozzle, then multi-3D components that have different geometry can be stacked with non-conformal mesh interfaces as is done in CATHARE 3. Table-1 shows how LOCA codes treat the momentum equations.

4. Discussions and Perspectives

The treatment of the momentum equations in the TRAC code may be not adequate to model the multi-dimensional component such as downcomer because it uses the phase intensive non-conservative form with finite difference discretization method. MARS Multi-D component also have the same approach. SPACE [7] uses the phase intensive modified non-conservative form with the equality eqn.(8). It may not be much different form TRACE.

Some study on this subject has been formed by CUPID group [4] by comparing the phase intensive non-conservative form with the mass weighted modified non-conservative (semi-conservative) form. The evidence was shown in the Fig.8.

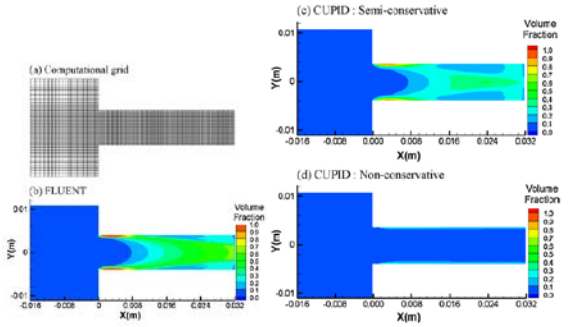

Fig.8. Effects of Momentum Convection Terms

As shown in Fig.8(c), mass weighted modified non-conservative form reasonably reproduces the result (Fig.8(b)) from FLUENT [14]. But the non-conservative form shows very different result (Fig8(d)). This study tells that the approach of TRACE is no good.

RELAP5 use mass weighted non-conservative form for sum equation and phase intensive form for difference equation [5]. This approach is better than the approach of TRACE. The lack of cross convection term is a weakness.

The rigorous conservative form of COBRA-TF is strongly recommended to handle the multi-dimensional multi-phase flow phenomena in the future. It is inevitable to develop the reasonable correlation for the covariance coefficients.

Finally, the finite volume discretization of the conservative momentum convection term is exemplified using the planar cylindrical cell in appendix for the pedagogical interests. The same procedure can be used to discretize the mass weighted modified non-conservative form of momentum equations.

REFERENCES

[1] B. Boyack. et. al., "Quantifying Reactor Safety Margins: Application of Code Scaling, Applicability, and Uncertainty Evaluation Methodology to a Large-Break, Loss of Coolant Accident", US.NRC, NUREG/CR-5249, 1989.
[2] M. Thurgood, et. al., "COBRA/TRAC: A Thermal Hydraulics Code for Transient Analysis of Nuclear Reactor Vessels and Primary Coolant Systems", US.NRC, NUREG/CR-3046, 1983.
[3] Spore, J.W., et al., TRAC-PF1/MOD2 Volume I Theory manual, NUREG/CR-5673, 1993, Los Alamos National Laboratory.
[4] Jeong, J.J. et al., 2008b. "A semi-implicit numerical scheme for transient two-phase flows on unstructured grids". NED 238, 3403–3412.
[5] MARS Code manual volume I: Code Structure, System Models, and Solution Methods KAERI/TR-2812/2004, December 2009, Korea Atomic Energy Research Institute.
[6] RELAP5/MOD3.3 Code manual, vol-I: Validation of numerical techniques in RELAP5/MOD3.0, Nuclear Safety Analysis Division, NUREG/CR-5535/Rev-1, December, 2001.
[7] S. J. Ha, C. E. Park, K. D. Kim, and C. H. Ban, "Development of the SPACE Code for Nuclear Power Plants", Nuclear Technology, Vol. 43, No. 1 (2011).
[8] I. Dor, et al., CATHARE 3D Module, Nureth-15, Pisa, Italy, May 12-17, 2013.
[9] J. W. Simons, 2D/3D Program, Work Summary Report, NUREG/IA-0126, MPR Associates, Inc. June 1993.
[10] S. Y. Lee, T. Hibiki, M. Ishii, "Formulation of time and volume averaged two-fluid model considering structural materials in a control volume", NED 239 (2009) 127–139.
[11] M. Ishii, T. Hibiki, Thermo-Fluid Dynamics of Two-Phase Flow, Second Edition, Springer, 2011.
[12] M. Ishii K. Mishima, "Two-fluid model and hydrodynamic constitutive relations". NED 82, (1984) 107-126.
[13] U.S. Nuclear Regulatory Commission, TRACE V5.0, Theory Manual, 2000.
[14] FLUENT Inc., 2006. FLUENT 6.3, User's Guide.
[15] H. Weller, "Derivation, modelling and solution of the conditionally averaged two-phase flow equations", Technical Report TR/HGW/02, Nabla Ltd, 2002.

Nomenclature

ϵ: porosity
α: volume fraction
ρ: density
$\boldsymbol{v}$: velocity
p: pressure
K: pressure drop coefficient
C_v: covariance coefficient
k: phase k

Appendix

Discretization of $\nabla \cdot (\boldsymbol{uu})$ in cylindrical cell using Finite Volume Method

With the following planar cylindrical cell (Fig.A-1), finite volume method can be applied to discretize the term $\nabla \cdot (\boldsymbol{uu})$ with a vector field $\boldsymbol{u} = u\boldsymbol{i}_r + v\boldsymbol{i}_\theta$. Especially the term $-\frac{v^2}{r}$ and the term $\frac{uv}{r}$ are automatically derived. Up-winding and splitting are also possible.

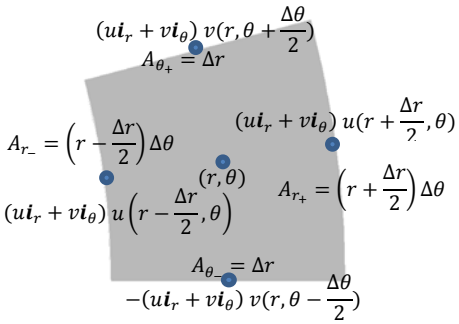

Fig.A-1. FVM discretization on Cylindrical Planar Cell

$$\int_{\text{cell}} \nabla \cdot \boldsymbol{uu} dV = \int_{\text{surf}} \boldsymbol{uu} \cdot d\boldsymbol{A} = \sum_s \boldsymbol{u} u_s A_s$$

$$= \begin{pmatrix} [(u\boldsymbol{i}_r + v\boldsymbol{i}_\theta)u]\left(r + \frac{\Delta r}{2}, \theta\right)\left(r + \frac{\Delta r}{2}\right)\Delta\theta \\ -[(u\boldsymbol{i}_r + v\boldsymbol{i}_\theta)u]\left(r - \frac{\Delta r}{2}, \theta\right)\left(r - \frac{\Delta r}{2}\right)\Delta\theta \\ +[(u\boldsymbol{i}_r + v\boldsymbol{i}_\theta)v]\left(r, \theta + \frac{\Delta\theta}{2}\right)\Delta r \\ -[(u\boldsymbol{i}_r + v\boldsymbol{i}_\theta)]v\left(r, \theta - \frac{\Delta\theta}{2}\right)\Delta r \end{pmatrix}$$

$$= \begin{pmatrix} \begin{pmatrix} [uu]\left(r + \frac{\Delta r}{2}, \theta\right)A_{r_+} \\ -[uu]\left(r - \frac{\Delta r}{2}, \theta\right)A_{r_-} \\ +[uv]\left(r, \theta + \frac{\Delta\theta}{2}\right)A_{\theta_+} \\ -[uv]\left(r, \theta - \frac{\Delta\theta}{2}\right)A_{\theta_-} \\ -\frac{[vv](r,\theta)}{r} r\Delta r\Delta\theta \end{pmatrix} \boldsymbol{i}_r(r,\theta) \\ + \begin{pmatrix} [vu]\left(r + \frac{\Delta r}{2}, \theta\right)A_{r_+} \\ -[vu]\left(r - \frac{\Delta r}{2}, \theta\right)A_{r_-} \\ +[vv]\left(r, \theta + \frac{\Delta\theta}{2}\right)A_{\theta_+} \\ -[vv]\left(r, \theta - \frac{\Delta\theta}{2}\right)A_{\theta_-} \\ +\frac{[uv](r,\theta)}{r} r\Delta r\Delta\theta \end{pmatrix} \boldsymbol{i}_\theta(r,\theta) \end{pmatrix}$$